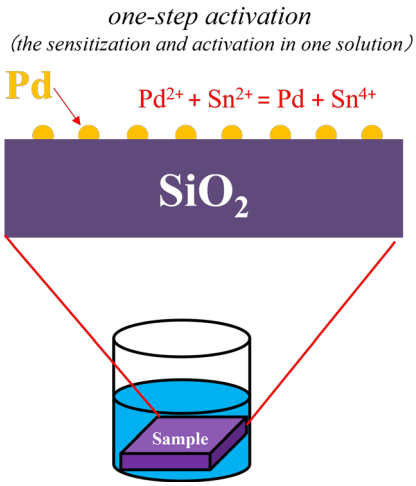

Fig. 1. Schematic diagram of Pd^{2+} reduction and deposition on SiO_2 in a colloidal wet process.

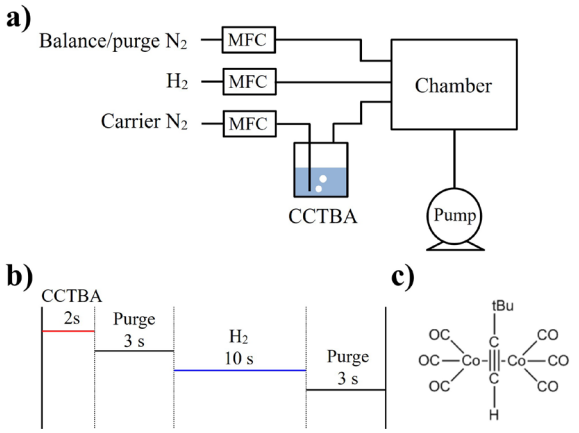

Fig. 3. Schematic illustration of the Co-ALD process: (a) ALD system used for Co deposition; (b) gas pulsing sequence employed during Co-ALD; (c) molecular structure of the Co precursor, dicobalt hexacarbonyl tert-butylacetylene (CCTBA).

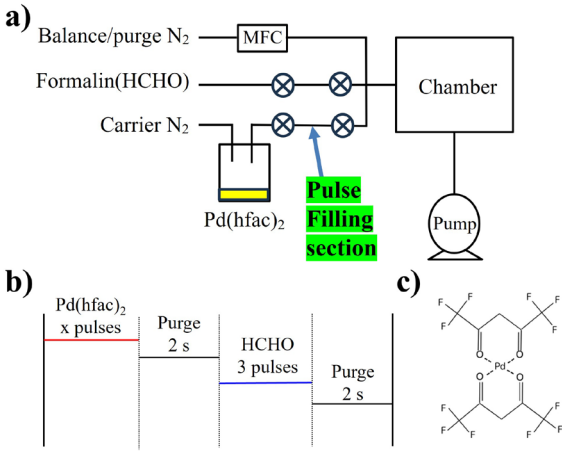

Fig. 2. Schematic illustration of the Pd-ALD process: (a) ALD system used for Pd activation; (b) gas pulsing sequence employed during Pd-ALD; (c) molecular structure of the Pd precursor, palladium(II) hexafluoroacetylacetonate ($Pd(hfac)_2$).

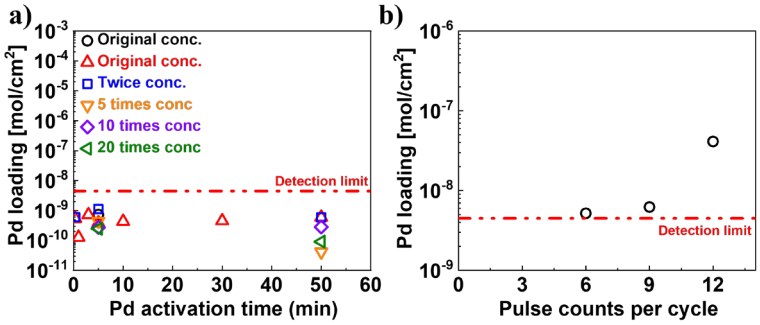

Fig. 4. Control of Pd loading via (a) variation of solution concentration and activation time in the wet process; (b) adjustment of precursor pulse counts per cycle in the ALD process.

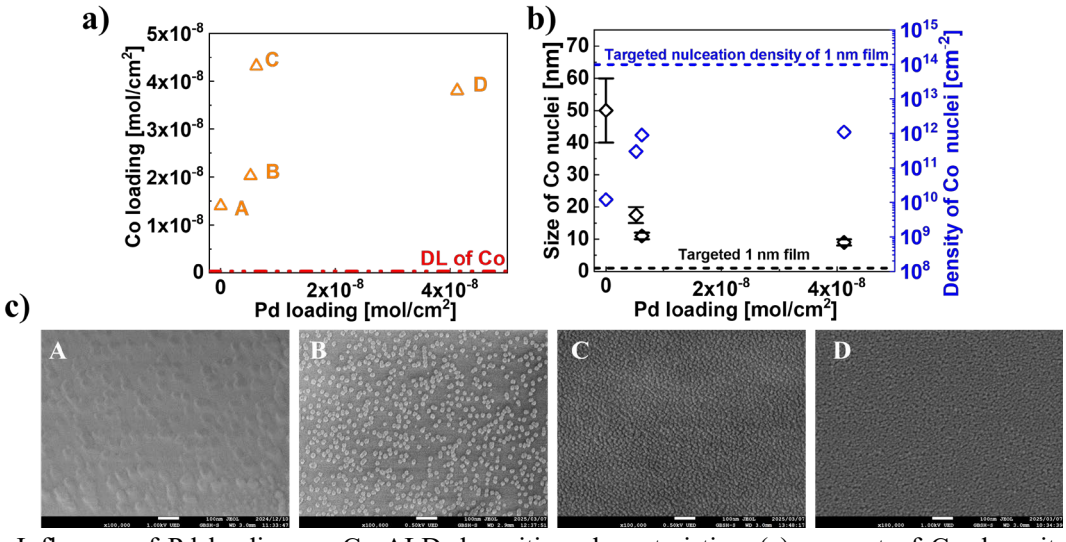

Fig. 5. Influence of Pd loading on Co-ALD deposition characteristics: (a) amount of Co deposited as a function of Pd loading; (b) variation in Co nuclei density and size with different Pd loadings; (c) surface morphology of Co films corresponding to the four Pd conditions shown in (a).